Inhibition of c-Jun N-terminal kinase signaling promotes osteoblastic differentiation of periodontal ligament stem cells and induces regeneration of periodontal tissues

兼子, 大志

Archives of Oral Biology 134 (2022) 105323

Contents lists available at ScienceDirect

Archives of Oral Biology

journal homepage: www.elsevier.com/locate/archoralbio

Inhibition of c-Jun N-terminal kinase signaling promotes osteoblastic differentiation of periodontal ligament stem cells and induces regeneration of periodontal tissues

Hiroshi Kaneko [a], Daigaku Hasegawa [b,*], Tomohiro Itoyama [b], Shinichiro Yoshida [b], Atsushi Tomokiyo [b], Sayuri Hamano [a,c], Hideki Sugii [a], Hidefumi Maeda [a,b]

[a] Department of Endodontology and Operative Dentistry, Faculty of Dental Science, Kyushu University, Fukuoka, Japan
[b] Division of Endodontology, Kyushu University Hospital, Kyushu University, Fukuoka, Japan
[c] Faculty of Dental Science, OBT Research Center, Kyushu University, Fukuoka, Japan

ARTICLE INFO

Keywords:
JNK inhibition
SP600125
Periodontal ligament stem cells
Osteoblastic differentiation
Periodontal tissue regeneration

ABSTRACT

Objectives: Few clinical treatments to regenerate periodontal tissue lost due to severe endodontic and periodontal disease have yet been developed. Therefore, the development of new treatment methods for the regeneration of periodontal tissue is expected. The purpose of this study was to investigate the effects of a c-Jun N-terminal kinase (JNK) inhibitor, SP600125, on the osteoblastic differentiation of periodontal ligament stem cells (PDLSCs) in vitro, and the function of SP600125 on the regeneration of alveolar bone in vivo.

Design: Alizarin red S staining, quantitative RT-PCR, and western blotting analysis was performed to determine whether SP600125 affects osteoblastic differentiation of human PDLSCs (HPDLSCs) and bone-related intracellular signaling. The effect of SP600125 on the regeneration of alveolar bone was assessed by using a rat periodontal defect model. The healing of periodontal defects was evaluated using micro-CT scans and histological analysis.

Results: SP600125 promoted the osteoblastic differentiation such as Alizarin red S-positive mineralized nodule formation and the expression of osteoblast-related genes in HPDLSCs under osteogenic conditions. In addition, this inhibitor upregulated the BMP2 expression and the phosphorylation of Smad1/5/8 in HPDLSCs under the same conditions. The inhibition of Smad1/5/8 signaling by LDN193189 suppressed the SP600125-induced osteoblastic differentiation of HPDLSCs. Furthermore, the application of SP600125 promoted the regeneration of not only alveolar bone but also PDL tissue in periodontal defects.

Conclusion: This study suggested that inhibition of JNK signaling promotes the osteoblastic differentiation of HPDLSCs through BMP2-Smad1/5/8 signaling, leading to the regeneration of periodontal tissues such as alveolar bone and PDL tissue.

1. Introduction

The destruction of periodontal tissues by severe endodontic and periodontal disease leads to loss of the affected teeth. Therefore, repairing or regenerating destroyed periodontal tissues is considered to be important for preserving teeth. Periodontal tissues comprise periodontal ligament (PDL), alveolar bone, cementum, and gingiva. Among them, the PDL cell population consists of various cell types, including fibroblasts, which are the principal cells in PDL tissue (Beertsen, McCulloch, & Sodek, 1997), osteoblasts, cementoblasts, and epithelial cell rests of Malassez (Freeman, 1994). Moreover, it has been revealed that PDL tissue includes multipotent PDL stem cells (PDLSCs)

Abbreviations: PDL, periodontal ligament; PDLSCs, PDL stem cells; JNK, c-Jun N-terminal kinase; HPDLSCs, human PDLSCs; α-MEM, alpha minimum essential medium; FBS, fetal bovine serum; PFA, paraformaldehyde; SDS, sodium dodecylsulfate; CM, control medium; DM, differentiation medium; RT-PCR, reverse transcription polymerase chain reaction; OSX, osterix; BSP, bone sialoprotein; OPN, osteopontin; BMP2, bone morphogenetic protein 2; micro-CT, microcomputed tomography; PBS, phosphate-buffered saline; H&E, hematoxylin and eosin; BSA, bovine serum albumin; RT, room temperature; DAPI, 4′,6-diamidino-2-phenylindole; SD, standard deviation.

* Corresponding author.
E-mail address: daigaku8@dent.kyushu-u.ac.jp (D. Hasegawa).

https://doi.org/10.1016/j.archoralbio.2021.105323
Received 18 August 2021; Received in revised form 31 October 2021; Accepted 23 November 2021
Available online 26 November 2021

that can differentiate into both osteoblasts and cementoblasts (Seo et al., 2004; Fujii et al., 2008). In the process of periodontal tissue regeneration, PDLSC was reported to form not only alveolar bone, but also PDL tissue owing to the appropriate formation of alveolar bone (Nagata et al., 2017; Iwasaki et al., 2019). These findings indicate that PDLSCs are responsible for the healing and repair of periodontal tissues through bone formation. Therefore, it is important to find factors to promote the regeneration of alveolar bone by PDLSCs for the therapeutic development of more effective periodontal tissue regeneration.

C-Jun N-terminal kinase (JNK) is a protein kinase activated by cytokines, growth factors, and environmental stress, and controls cell proliferation, differentiation, apoptosis, survival, and the inflammatory response (Chen, Meyer, & Tan, 1996; Guo, Baysal, Kang, Yang, & Williamson, 1998; Davis, 2000; Kyriakis & Avruch, 2001; Weston & Davis, 2002). A previous report showed that, in PDL tissue, mechanical strains caused by occlusion and mastication promote JNK-phosphorylation of PDL fibroblasts (Papadopoulou, Iliadi, Eliades, & Kletsas, 2017). JNK is known to be associated with cancer and autoimmune diseases, and animal studies have already shown that JNK inhibitors have therapeutic effects on ovarian cancer and multiple sclerosis (Ichiyama et al., 2011; Seino et al., 2016). We recently reported that JNK is involved in Wnt5a-induced suppression of the osteoblastic differentiation of HPDLSCs (Hasegawa et al., 2018). Other previous reports showed that JNK inhibitor induces the osteoblastic differentiation of undifferentiated cells (Huang, Lin, Lin, Su, & Hung, 2012; Guo, Wang, Xu, Wang, & Song, 2015). These findings indicate that JNK inhibition may play an important role in regulating osteoblastic differentiation or bone formation. However, the effect of JNK inhibition on the osteoblastic differentiation of PDLSCs or regeneration of damaged periodontal tissues remains unclear.

Therefore, in this study, we examined the effect of JNK inhibition on the osteoblastic differentiation of PDLSCs and the involved signaling molecules, and the effect of a JNK inhibitor on the regeneration of alveolar bone in periodontal defects.

2. Materials and methods

2.1. Reagents

SP600125, a JNK inhibitor, was purchased from Wako Pure Chemical Industries Ltd. (Osaka, Japan). LDN193189, Smad1/5/8 inhibitor, was purchased from MedChemExpress (Monmouth Junction, NJ).

2.2. Cell culture

An immortalized human PDL cell line (2–23 cells), which showed high growth capacity, multipotency, and the expression of stem cell-related surface markers in our previous study (Hasegawa et al., 2018), was used as human PDL stem cells (HPDLSCs). 2–23 cells were cultured in alpha minimum essential medium (α-MEM; Gibco-BRL, Grand Island, NY) containing 10% fetal bovine serum (FBS; Biosera, Nuaillé, France; 10% FBS/α-MEM) supplemented with 50 μg/mL streptomycin and 50 U/mL penicillin (Gibco-BRL) at 37 °C in a humidified atmosphere of 5% CO2 and 95% air. All procedures were performed in compliance with the requirements of Kyushu University Medical District Department Clinical Research Ethics Committee.

2.3. Cell viability assay

2–23 cells (5×10^3 cells per well) were cultured in 10% FBS/α-MEM with 0, 1, 10, 50, 100 μM SP600125, or 0, 1, 10, 50, 100 nM LDN193189 in 48-well plates (Becton Dickinson Labware, Lincoln Park, NJ) in 250 μl of culture medium per well for 1, 2, or 3 days. SP600125 or LDN193189 were added at 24 h after cell seeding. At 0, 1, 2, and 3 days, viable cells were measured using a Cell Proliferation Assay kit (Merck Millipore, Darmstadt, Germany), as described previously (Hasegawa et al., 2020). Briefly, at the indicated time points, 25 μl of kit reagent, WST-1, was added to the culture medium of each well. After 1 h, 100 μl of supernatant was collected from each well, and the density was measured at absorbance of 450 nm using a microplate reader (ImmunoMini NJ-2300; System Instruments Co., Ltd., Tokyo, Japan).

2.4. Osteoblastic differentiation assay

2–23 cells were seeded at 1×10^4 cells per well in 24-well plates (Becton Dickinson Labware) in 10% FBS/α-MEM as control medium (CM), CM containing 2 mM β-glycerophosphate (Sigma Aldrich, St. Louis, MO), 50 mg/mL ascorbic acid (Nacalai Tesque, Kyoto, Japan), and 10^{-7} M dexamethasone (Merck Millipore) as osteoblastic differentiation medium (DM) (Maeda, Wada, Nakamuta, & Akamine, 2004). SP600125 and/or LDN193189 were added at the same time as the start of stimulation with DM (when the cells are subconfluent after seeding). Half of the medium in each well was exchanged every 2 days. After 2 weeks of culture, the cells were fixed with 4% paraformaldehyde (PFA; Merck Millipore) and then washed with distilled water and exposed to Alizarin red S (Sigma Aldrich) stain as described previously (Hasegawa et al., 2015). The area of each Alizarin red S-positive region was imaged and measured using a Biozero digital microscope (Keyence Corporation, Osaka, Japan).

2.5. Western blotting analysis

The cells were lysed in a buffer containing 50 mM Tris-HCl, pH 6.9 (Sigma Aldrich), 2% sodium dodecylsulfate (SDS; Nacalai Tesque), 6% 2-mercaptoethanol (Sigma Aldrich), and 10% glycerol. Aliquots containing 20 μg of protein per lane were subjected to 4–20% SDS polyacrylamide gel electrophoresis and subsequently transferred onto an Immuno-Blot PVDF membrane (Bio-Rad Laboratories, Hercules, CA). This membrane was reacted with rabbit polyclonal anti-p-JNK (Cell Signaling Technology, Beverly, MA) at a dilution of 1:500, rabbit polyclonal anti-JNK (Cell Signaling Technology) at a dilution of 1:500, rabbit polyclonal anti-p-Smad1/5/8 (Abcam, Cambridge, UK) at a dilution of 1:500, rabbit polyclonal anti-Smad1/5/8 (Santa Cruz Biotechnology, CA) at a dilution of 1:500, rabbit monoclonal anti-p-ERK1/2 (Cell Signaling Technology) at a dilution of 1:1000, rabbit polyclonal anti-ERK1/2 (Cell Signaling Technology) at a dilution of 1:1000, rabbit polyclonal anti-BMP2 (ProteinTech Group, Chicago, IL) at a dilution of 1:1000, or mouse monoclonal anti-β-actin (Santa Cruz Biotechnology) at a dilution of 1:1000. The reactions were followed using biotinylated anti-mouse IgG (Nichirei Biosciences, Inc., Tokyo, Japan) or anti-rabbit IgG (Nichirei Biosciences). The reactive bands were visualized using ECL Prime Western blotting detection system (GE Healthcare, Little Chalfont, UK). As the standard protein ladder, Full-Range Rainbow Molecular Weight Markers (GE Healthcare) and BLUeye Prestained Protein Ladder (GeneDireX Inc., Las Vegas, NV) were used. Relative expression levels of each protein were quantified using ImageJ software (National Institutes of Health).

2.6. Quantitative reverse transcription polymerase chain reaction (RT-PCR)

Total cellular RNA was isolated with TRIzol Reagent (Invitrogen, Carlsbad, CA), in accordance with the manufacturer's instructions. First-strand cDNA was synthesized from 1 μg of total RNA using an ExScript RT Reagent kit (Takara Bio Inc., Kusatsu, Japan). Total RNA was reverse-transcribed with random 6-mers and ExScript RTase for 15 min at 42 °C, and the reaction was stopped by incubation for 2 min at 99 °C, followed by 5 min at 5 °C. PCR was performed using KAPA Express Extract (Kapa Biosystems, Woburn, MA) in a Thermal Cycler Dice Real Time System (Takara Bio Inc.) under the following conditions: 95 °C for 10 s, then 40 cycles at 95 °C for 5 s and 60 °C for 30 s, followed by a dissociation protocol at 95 °C for 15 s, 60 °C for 30 s, and 95 °C for 15 s.

Primer sequences, annealing temperatures, cycle numbers, and product sizes for *osterix* (*OSX*), *bone sialoprotein* (*BSP*), *osteopontin* (*OPN*), *bone morphogenetic protein 2* (*BMP2*), and *β-actin* are shown in Table 1. β-actin primers were used as internal standards. Expression levels of the target genes were calculated using the 2ˆ(-ΔΔCt) values.

2.7. Application of JNK inhibitor in a rat periodontal defect model

Eight-week-old male Wistar rats (Kyudo, Saga, Japan) were used to develop a rat periodontal defect model. After the rats had been anesthetized by the injection of 2.5 mg/kg butorphanol tartrate (Meiji Seika Pharma, Tokyo, Japan), 0.15 mg/kg medetomidine hydrochloride (Kyoritsu Seiyaku, Tokyo, Japan), and 2 mg/kg midazolam (Fuji Seiyaku Kogyo, Tokyo, Japan), the periodontal defect was surgically created by a modified version of the method reported by King, King, Cruchley, Wozney, & Hughes (1997). Briefly, an extraoral incision was made at the buccal side of the mandible and the buccal plate was exposed. Then, the buccal alveolar bone, PDL, and part of the cementum and dentin corresponding to the distal root of the mandible first molar to the mesial root of the second molar were removed to create a periodontal defect using dental round burs #6 (MANI, Tochigi, Japan). Each periodontal defect in the buccal area was 1.5 mm in height and 2.0 mm in width. After creation of the defect, 10 mM (17.6 μg) of SP600125 or DMSO (as controls) was applied into the defect with an atelocollagen honeycomb sponge (Koken, Tokyo, Japan). The masseter and skin were sutured with 5–0 nylon and 3–0 silk (MANI). This experiment was performed using 8 rats (N = 8). In each rat, one side is set as the experimental group and the other side as the control group. For 4 of the 8 rats, the right side was set as the experimental group and the left side as the control group, and the other 4 rats had the opposite. Rats were allowed free access to food and water throughout the experimental period. All procedures were performed with approval from the Animal Ethics Committee and followed the regulations of Kyushu University.

2.8. Microcomputed tomography (micro-CT) analysis

Two weeks after application, the healing of periodontal defects was evaluated using micro-CT scans (SkyScans 1076; Bruker Micro-CT, Kontich, Belgium). Three-dimensional image construction was performed using NRecon (Bruker, Billerica, MA).

2.9. Histological analysis

Two or four weeks after application, rats were transcardially perfused with 4% PFA (Merck Millipore) in phosphate-buffered saline (PBS) under anesthesia, as mentioned above. Mandibular specimens were extracted and immersed in 4% PFA for an additional 24 h. These were then washed with PBS and decalcified in 10% ethylenediaminetetraacetic acid (Nacalai Tesque) at 4 °C for 4 weeks before dehydration and embedding in paraffin. The embedded samples were then sectioned (5 μm in thickness). The sections were observed microscopically using a BZ800 apparatus (Keyence Corporation) after hematoxylin and eosin, Masson's trichrome, or immunofluorescence/histochemical staining.

2.10. Immunofluorescence staining

The sections were deparaffinized and nonspecific antigens were blocked with 2% bovine serum albumin (BSA; Nacalai Tesque) in PBS for 1 h at room temperature (RT). A rabbit polyclonal anti-osterix antibody (1:1000 dilution; Abcam), a mouse monoclonal anti-scleraxis antibody (1:25 dilution; Santa Cruz Biotechnology), a normal rabbit IgG antibody (1:1000 dilution; Cell Signaling Technology), or a normal mouse IgG antibody (1:25 dilution; Cell Signaling Technology) were applied as the primary antibody overnight at 4 °C. Sections were then incubated with an Alexa 568-conjugated goat anti-rabbit IgG secondary antibody (1:200 dilution; Invitrogen) or an Alexa 488-conjugated chicken anti-rabbit IgG secondary antibody (1:200 dilution; Invitrogen) for 30 min at RT. Subsequently, sections were counterstained with 4′,6-diamidino-2-phenylindole (DAPI; Vector Laboratories, Burlingame, CA). The tissue was imaged and analyzed using a Biozero digital microscope (Keyence Corporation).

2.11. Immunohistochemical staining

The sections were deparaffinized and nonspecific antigens were blocked with 2% BSA in PBS for 1 h at RT. A rabbit polyclonal anti-periostin antibody (1:1000 dilution; Santa Cruz Biotechnology) was applied as the primary antibody overnight at 4 °C. Sections were then incubated with biotinylated anti-rabbit IgG (Nichirei Biosciences) as the secondary antibody at RT for 30 min, followed by an avidin-peroxidase conjugate (Nichirei Biosciences) for 30 min at RT. Positive staining was visualized using Simple Stain DAB solution (Nichirei Biosciences). Staining of nuclei was performed using Mayer's hematoxylin solution (Wako Pure Chemical Industries Ltd.).

2.12. Statistical analysis

All data was analyzed at least three times and expressed as the mean ± standard deviation. Statistical analysis was performed by one-way ANOVA followed by the Benjamini–Hochberg method for multiple comparisons. Student's paired *t*-test was performed for comparisons of two mean values. Differences were considered significant at $P < 0.05$. In all experiments, the normality of the data distribution is first validated by the Shapiro-Wilk normality test before performing one-way ANOVA or *t*-test.

Table 1
Primer sequences, annealing temperatures, cycle numbers, and product sizes for quantitative RT-PCR.

Gene (abbreviation)	GenBank ID	Primer sequence forward/reverse	Annealing temperature (°C)	Quantitative RT-PCR (cycles)	Size of amplified products (bp)
OSX	NM_152860.2	5′-GCCATTCTGGGCTTGGGTATC-3′/5′-GAAGCCGGAGTGCAGGTATCA-3′	60	40	129
BSP	NM_004967.4	5′-CTGGCACAGGGTATACAGGGTTAG-3′/5′-ACTGGTGCCGTTTATGCCTTG-3′	60	40	182
OPN	NM_001040058.2	5′-ACACATATGATGGCCGAGGTGA-3′/5′-TGTGAGGTGATGTCCTCGTCTGT-3′	60	40	115
BMP2	NM_001200.4	5′-TCCACTAATCATGCCATTGTTCAGA-3′/5′-GGGACACAGCATGCCTTAGGA-3′	60	40	74
β-actin	NM_001101.5	5′-ATTGCCGACAGGATGCAGA-3′/5′-GAGTACTTGCGCTCAGGAGGA-3′	60	40	89

3. Results

3.1. Endogenous JNK and phosphorylated JNK are expressed in HPDLSCs

In this study, 2–23 cells were initially examined for the expression of JNK by western blotting analysis. The results showed that this cell line clearly expressed endogenous JNK and phosphorylated JNK (Supplementary Fig. 1A). Next, the effect of SP600125 on the cell viability of 2–23 cells was examined. Cell viability assay demonstrated that SP600125 did not adversely affect the cell viability at concentrations below 10 μM (Supplementary Fig. 1B).

3.2. JNK inhibition promotes osteoblastic differentiation of HPDLSCs

Western blotting analysis confirmed that the phosphorylation of JNK was decreased in 2–23 cells cultured in DM with SP600125 (Supplementary Fig. 1C, D). Based on these preliminary experiments, the effect of SP600125 on the osteoblastic differentiation of 2–23 cells was investigated. The results showed that this inhibitor increased Alizarin red S-positive areas compared with that with the SP600125-free culture, especially at a concentration of 10 μM (Fig. 1A, B). In addition, quantitative RT-PCR also demonstrated that the expression levels of osteoblast-related genes such as *OSX*, *BSP*, and *OPN* were significantly increased in 2–23 cells cultured in DM with SP600125 (Fig. 1C–E). These results indicated that JNK inhibition promoted the osteoblastic differentiation of HPDLSCs.

3.3. JNK inhibition activates Smad1/5/8 signaling in HPDLSCs

To clarify the intracellular signaling molecules that are involved in mediating the promotive effect of JNK inhibition on the osteoblastic differentiation of HPDLSCs, we examined the effects of JNK inhibition on the phosphorylation of bone-related intracellular signaling molecules such as Smad1/5/8 (Rath et al., 2011) and ERK1/2 (Ge, Xiao, Jiang, & Franceschi, 2007) in HPDLSCs. Western blotting analysis showed that the phosphorylation of Smad1/5/8 was upregulated in 2–23 cells cultured in DM with SP600125 (Fig. 2A, B). In contrast, SP600125 treatment did not affect the phosphorylation of ERK1/2 in 2–23 cells (Fig. 2A, C). Furthermore, we examined the effect of SP600125 on the gene expression of *BMP2*, which is known to activate Smad1/5/8 signaling (Miyazono, Maeda, & Imamura, 2005), in HPDLSCs. It was found that the expression of BMP2 gene (Fig. 2D) and protein (Fig. 2E, F) in 2–23 cells was increased by SP600125 treatment, similar to upregulation of the Smad1/5/8 phosphorylation. These results indicated that JNK inhibition activated Smad1/5/8 signaling in HPDLSCs under osteogenic conditions.

3.4. Smad1/5/8 signaling is involved in JNK inhibition-induced promotion of osteoblastic differentiation of HPDLSCs

We next examined whether Smad1/5/8 signaling is involved in JNK inhibition-induced promotion of osteoblastic differentiation of HPDLSCs using a Smad1/5/8 inhibitor, LDN193189. Cell viability assay demonstrated that LDN193189 did not adversely affect the cell viability at concentrations below 100 nM (Supplementary Fig. 1E). Western

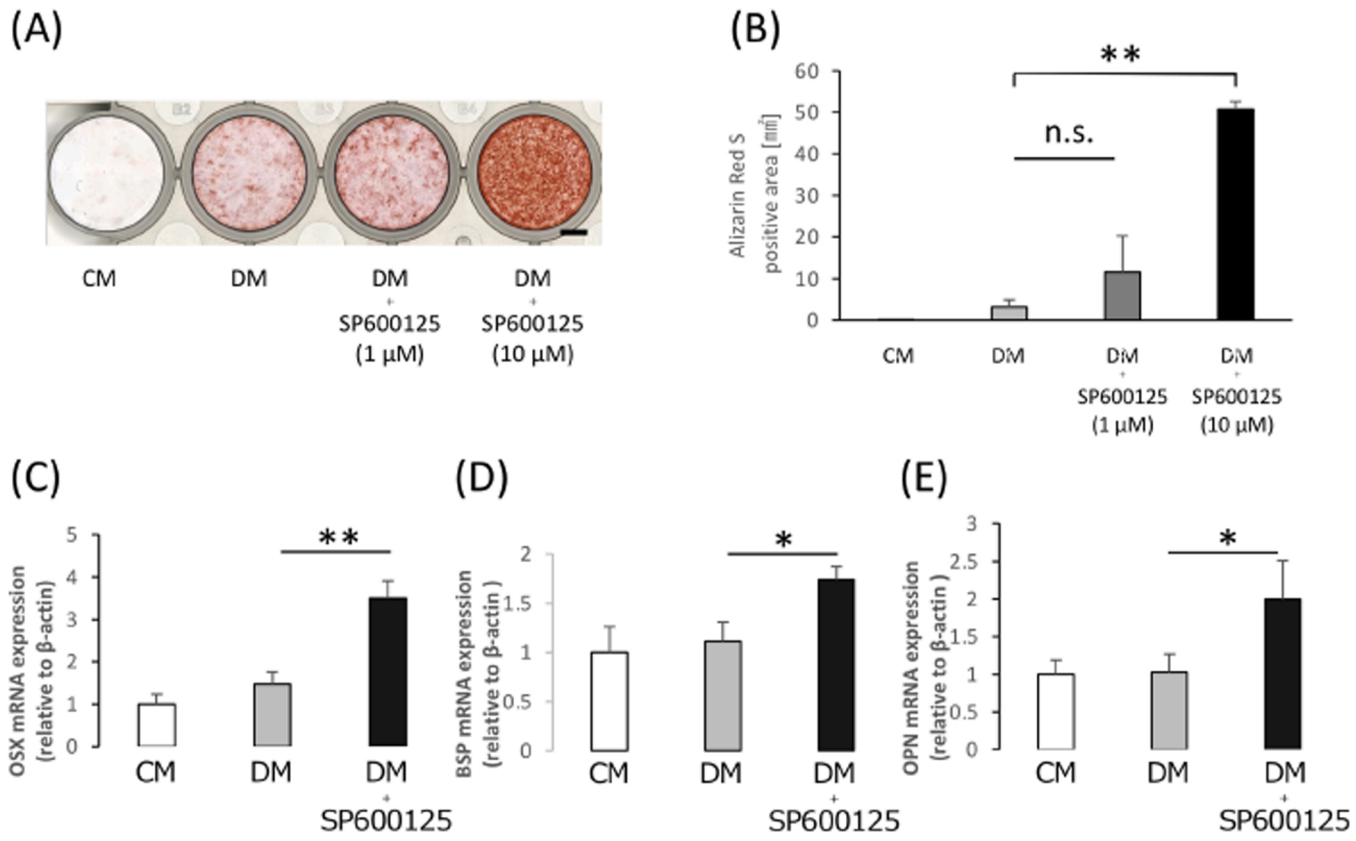

Fig. 1. Effects of JNK inhibition on osteoblastic differentiation of HPDLSCs. (A, B) Alizarin red S staining of 2–23 cells cultured in control medium (CM), osteoblastic induction medium (differentiation medium [DM]), and DM with 1 or 10 μM SP600125 (DM+SP600125 (1 μM) or DM+SP600125 (10 μM)) for 2 weeks (bars = 5 mm) (A). The graph shows quantitative analysis of the area of each Alizarin red S-positive region, which was imaged and measured using a Biozero digital microscope (B). (C–E) Quantitative RT-PCR was performed to analyze the gene expression of *OSX* (C), *BSP* (D), and *OPN* (E) in 2–23 cells cultured in CM, DM, and DM with 10 μM SP600125 (DM+SP600125) for 7 days. Data were all presented as mean ± standard deviation (error bars) for four individual experiments. **P < 0.01, *P < 0.05. n.s.: not significant.

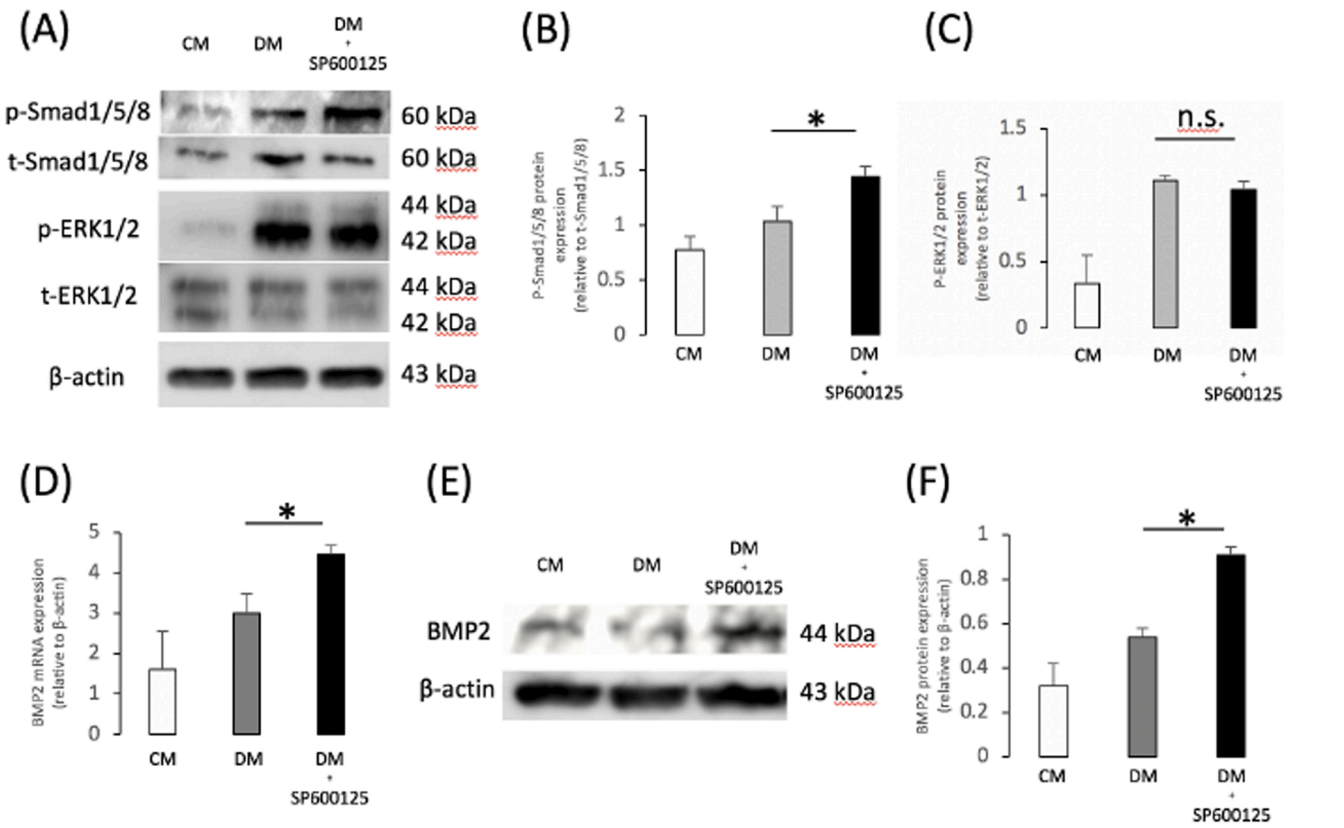

Fig. 2. Effects of JNK inhibition on intracellular signaling molecules in HPDLSCs. (A–C) 2–23 cells were cultured in CM, DM, or DM with 10 μM SP600125 (DM+SP600125) for 4 h. Western blotting analysis was performed to determine the expression of phosphorylated-Smad1/5/8 (p-Smad1/5/8), total-Smad1/5/8 (t-Smad1/5/8), phosphorylated-ERK (p-ERK), total-ERK (t-ERK), and β-actin was used as loading controls (A). The graphs show quantification of the expression of p-Smad1/5/8 (B), p-ERK (C). (D) Quantitative RT-PCR was performed to analyze the gene expression of *BMP2* in 2–23 cells cultured in CM, DM, and DM+SP600125 for 3 h. (E, F) Western blotting analysis was performed to analyze the protein expression of BMP2 in 2–23 cells cultured in CM, DM, and DM+SP600125 for 4 h, and β-actin was used as loading controls (E). The graphs show quantification of the protein expression of BMP2 (F). Data were all presented as mean ± standard deviation (error bars) for three individual experiments. *P < 0.05. n.s.: not significant.

blotting analysis confirmed that the phosphorylation of Smad1/5/8 was downregulated in 2–23 cells cultured in DM containing SP600125 with LDN193189 (Supplementary Fig. 1F, G). LDN193189 treatment suppressed SP600125-induced promotion of Alizarin red S-positive reaction (Fig. 3A, B) and upregulation of osteoblast-related genes expression in 2–23 cells (Fig. 3C-E). These results indicated that Smad1/5/8 signaling was involved in JNK inhibition-induced promotion of osteoblastic differentiation of HPDLSCs.

3.5. Application of JNK inhibitor promotes regeneration of alveolar bone in periodontal defects

We assessed the effects of JNK inhibition on the regeneration of bone tissue by using a rat periodontal defect model. The periodontal defects were surgically created by a modified version of the procedure described in a previous report (King et al., 1997). The buccal alveolar bone, PDL, and part of the cementum and dentin corresponding to the distal root of the mandibular first molar to the mesial root of the second molar were carefully removed to create periodontal defects (Fig. 4A, B). An atelocollagen sponge as a scaffold with or without SP600125 was placed into the defect (Fig. 4C). Two weeks after the operation, micro-CT images showed that, in the group with the application of SP600125, bone regeneration increased in the defect site compared with that in the control (Fig. 5A–D). We also investigated the structures of the regenerated alveolar bone in histological sections. The results demonstrated that, upon the application of SP600125, the bone volume was significantly higher than that in the control group (Fig. 5E–I). In addition, immunohistochemical staining demonstrated that the expression of osterix, which is one of the osteoblast-related markers, was stronger in the newly formed alveolar bone in the SP600125 group than in the control group (Fig. 5J-M, and Supplementary Fig. 2A-D). These results indicated that the JNK inhibitor promoted the regeneration of alveolar bone in periodontal defects.

3.6. Application of JNK inhibitor induces regeneration of PDL tissue in periodontal defects

Furthermore, we assessed whether JNK inhibition also affects the regeneration of PDL tissue. At 2 weeks after the SP600125 application, narrow spaces of connective tissue similar to PDL were formed adjacent to the newly formed bone in both groups, and these new tissues showed periodontal tissue-like structures (Fig. 5E-H). Masson's trichrome staining demonstrated that, at 2 weeks after the operation, the fibers in the control group were sparsely formed, irregular in orientation, and almost not attached to the root surface (Fig. 6A, C). On the other hand, the fibers in the SP600125 group were abundant and oriented generally perpendicularly on the root surface, although there were some gaps between the fibers and the root (Fig. 6B, D). Even at 4 weeks after the operation, the fibers in the control group remained parallel to the root and irregularly oriented (Fig. 6E, G), whereas the fibers in the SP600125 group were embedded into a thin layer on the root surface and oriented perpendicularly on the root surface, and exhibited the structure of "Sharpey's fibers" (Fig. 6F, H). In addition, the newly formed PDL tissue in the SP600125 group showed higher expression of PDL-related marker such as periostin (Fig. 6I, J) and scleraxis (Supplementary Fig. 2E-H), compared to that in the control group. These results indicated that the

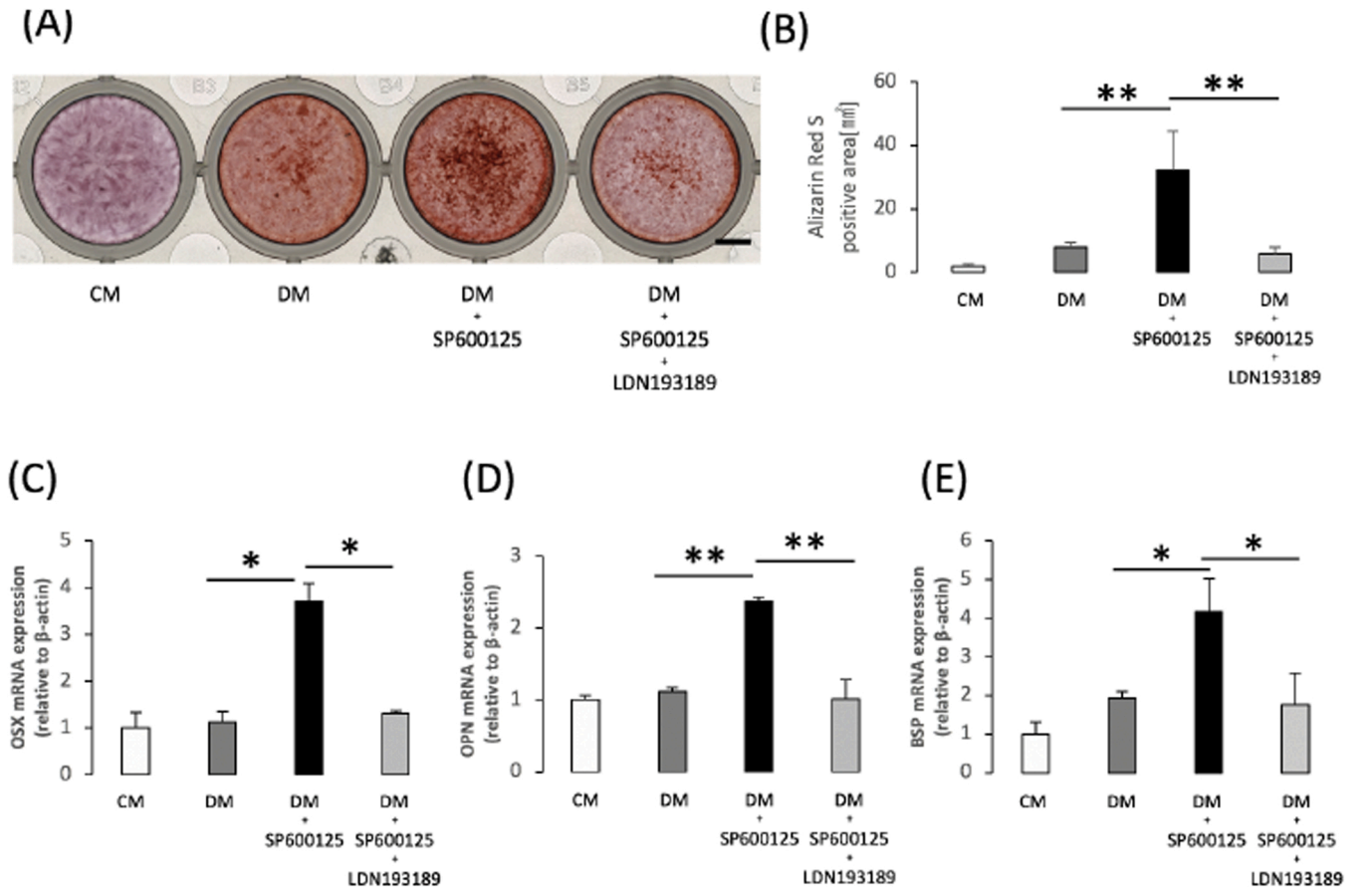

Fig. 3. The Role of Smad1/5/8 signaling on JNK inhibition-induced promotion of osteoblastic differentiation of HPDLSCs. (A-B) Alizarin red S staining of 2–23 cells cultured in CM, DM, and DM+SP600125 containing DMSO (DM+SP) or 100 nM LDN193189 (DM+SP+LDN) for 2 weeks (Bars = 5 mm) (A). The graph shows the quantitative analysis of the area of each Alizarin red S-positive region, which was imaged and measured using a Biozero digital microscope (B). (C-E) Quantitative RT-PCR was performed to analyze the gene expression of *OSX* (C), *BSP* (D), and *OPN* (E) in 2–23 cells cultured in CM, DM, DM+SP, and DM+SP+LDN for 7 days. Data were all presented as mean ± standard deviation (error bars) for four individual experiments. *P < 0.05. n.s.: not significant.

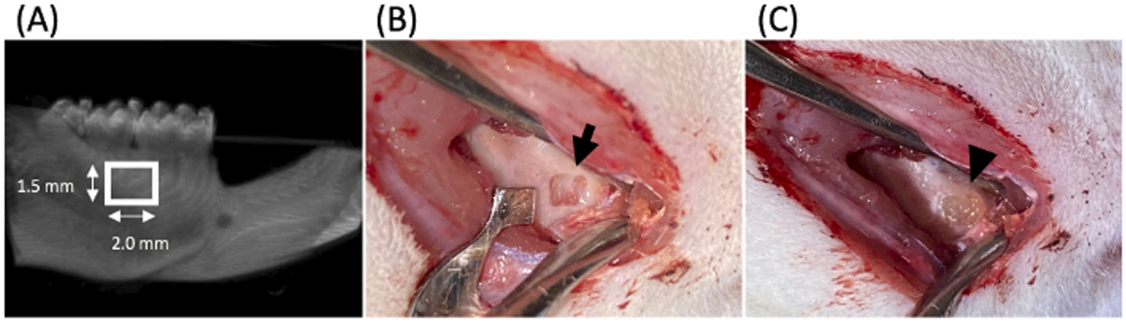

Fig. 4. Rat periodontal defect model. (A–C) Creation of rat periodontal defects and application of SP600125. (A) A micro-CT image of the buccal area of the mandibular bone before creating periodontal defects. White box represents the location and range of defects (height: 1.5 mm; width: 2.0 mm). (B) An image of the surgically created periodontal defects before the application of SP600125. Black arrow shows the location of defects. (C) An image of the application of SP600125 into periodontal defects with atelocollagen honeycomb sponges. Black arrowhead shows an atelocollagen honeycomb sponge. This experiment was performed using 8 rats (N = 8).

JNK inhibitor promoted the regeneration of not only alveolar bone but also PDL tissue.

4. Discussion

In the present study, we found that JNK inhibition promoted the osteoblastic differentiation of HPDLSCs in vitro and that JNK inhibitor induced the regeneration of alveolar bone and PDL tissue in a rat periodontal defect model. This is the first report to demonstrate that JNK inhibition can be a therapeutic target for the regeneration of periodontal tissues.

In order to establish a therapeutic method for the regeneration of lost periodontal tissues, the development of periodontal tissue regeneration methods using several bioactive molecules has been attempted so far. In addition to fibroblast growth factor (FGF), which has already been clinically applied (Takayama, Murakami, Shimabukuro, Kitamura, &

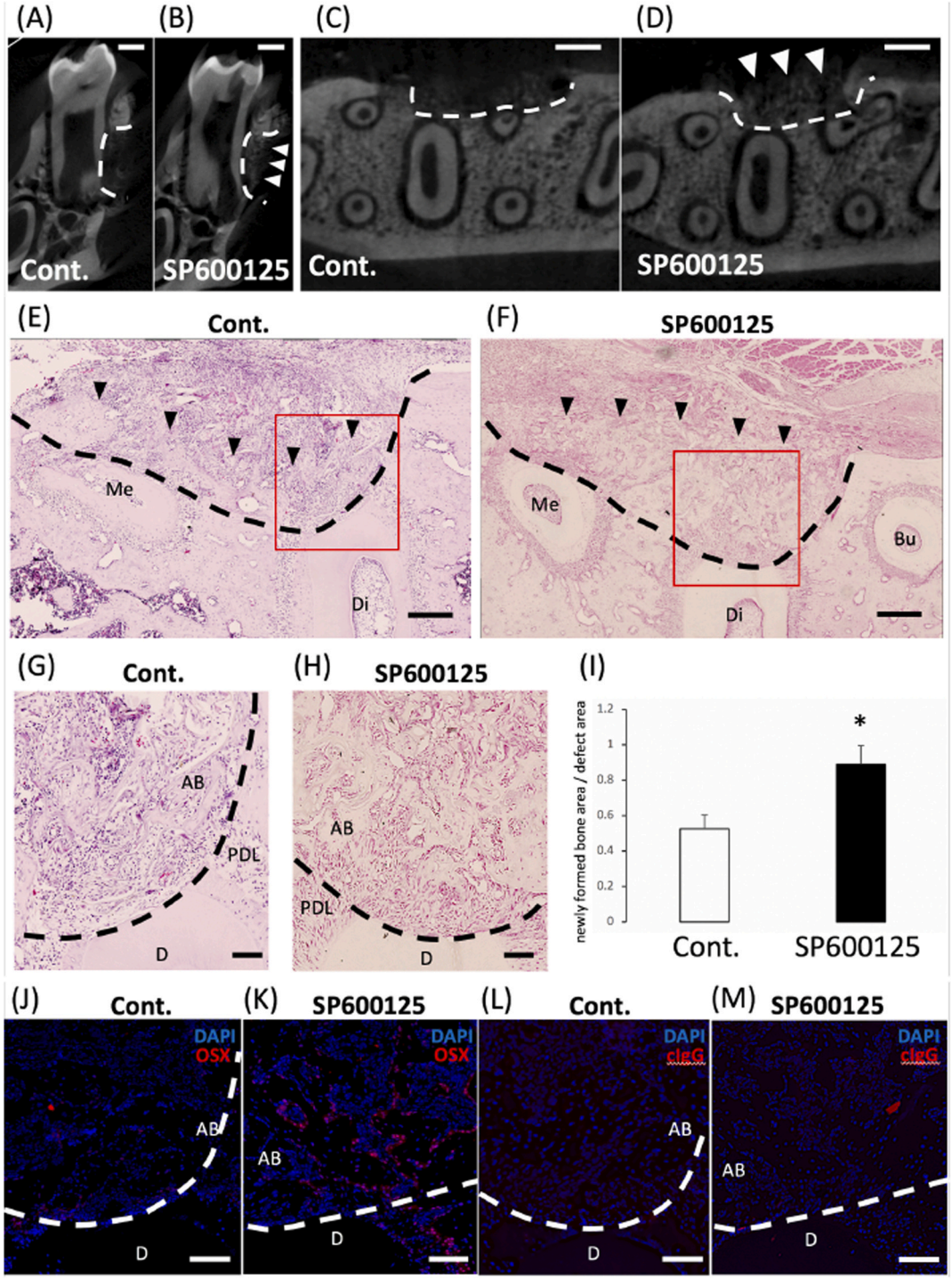

Fig. 5. Effects of JNK inhibitor on regeneration of alveolar bone in a rat periodontal defect model. (A–D) Representative 3D reconstructed micro-CT images of periodontal defects 2 weeks after the operation with the application of DMSO as a vehicle control (Cont.) (A, C) and SP600125 (B, D). Images are shown using long axial (A, B) and horizontal (C, D) sections. White dotted lines outline periodontal defects. White arrowhead shows the regenerated bone tissue. Bars = 500 μm. (E–I) Histological analyses in a rat periodontal defect model. Hematoxylin-eosin staining was performed to assess the formation of new alveolar bone in periodontal defects 2 weeks after the operation in the control group (Cont.) (E, G) and the SP600125 group (SP600125) (F, H). Black dotted lines outline periodontal defects. Black arrowhead shows the regenerated alveolar bone. Bars = 300 μm (E, F). Higher-magnification images focused on newly formed periodontal tissues near the root (G, H; red boxes in E and F). Bars = 100 μm. The graph shows the quantification of areas of eosin-positive regenerated alveolar bone in each group. Data were all presented as mean ± standard deviation (error bars) for three individual experiments. *$P < 0.05$. (I). (J–M) Immunofluorescence staining was performed to assess the expression of osterix (OSX; red) in the regenerated alveolar bone in Cont. (J) and SP600125 (K). No positive staining was observed in tissues incubated with rabbit control IgG (cIgG; L, M). White dotted lines outline periodontal defects. Cells were counterstained with DAPI (blue). Bars = 100 μm. All images are shown using horizontal sections, and are representatives of eight independent experiments. Me, the mesial root of the second molar; Di, the distal root of the first molar; Bu, the proximal buccal root of the first molar; AB, alveolar bone; D, dentin; PDL, periodontal ligament.

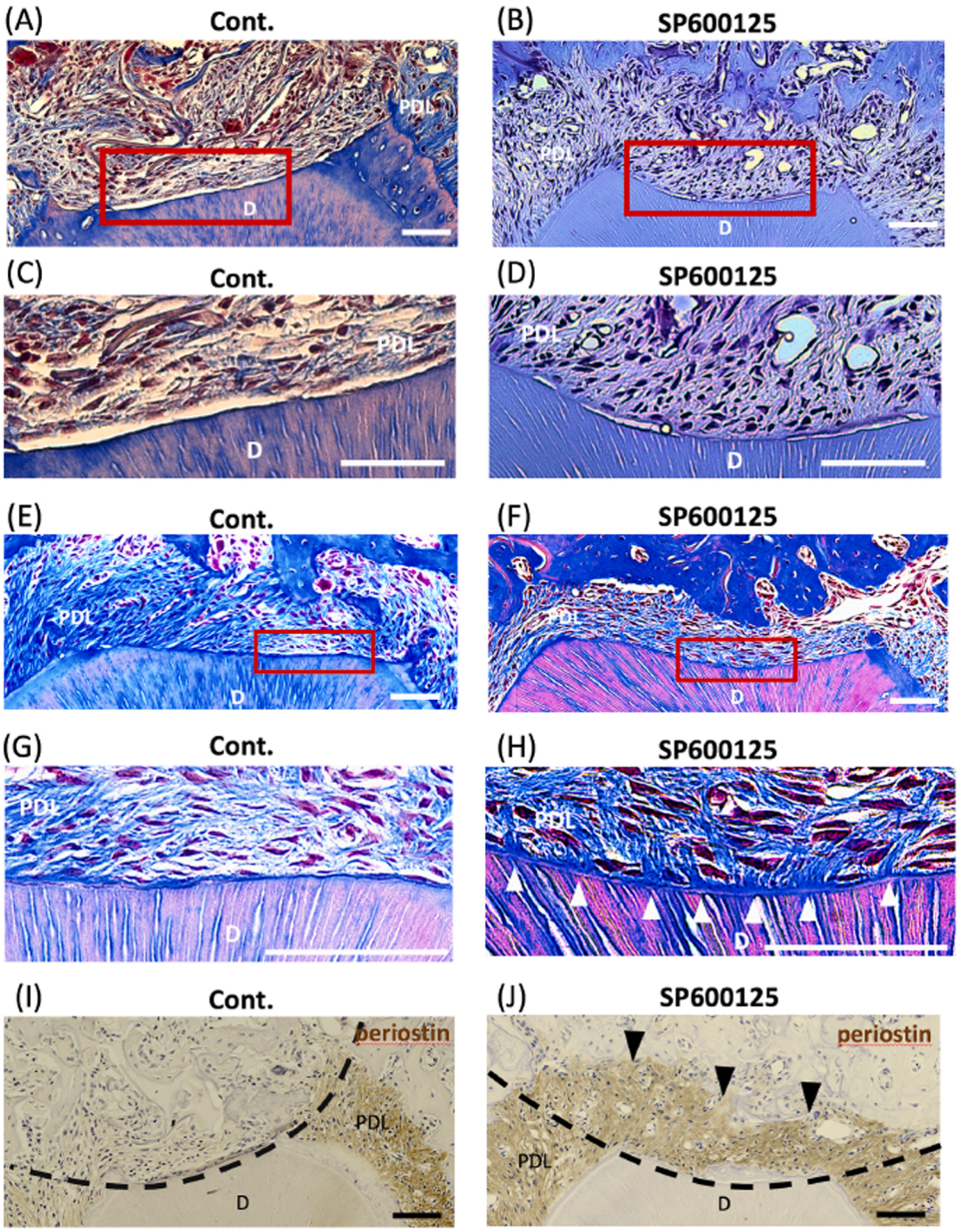

Fig. 6. Effects of JNK inhibitor on regeneration of PDL tissue in a rat periodontal defect model. (A–H) Masson's trichrome staining was performed to assess the formation of new PDL tissue in periodontal defects 2 weeks (A–D) and 4 weeks (E–H) after the operation in the control group (Cont.) (A, C, E, G) and the SP600125 group (SP600125) (B, D, F, H). Higher-magnification images focused on newly formed PDL tissue near the root (C, D, G, H; red boxes in A, B, E, F). White arrowhead shows the PDL fibers attached to a thin layer on the root surface (H). Bars = 100 μm. (I, J) Immunohistochemical staining was performed to assess the expression of periostin in newly formed PDL-like tissues in Cont. (I) and SP600125 (J). Black dotted lines outline periodontal defects. Black arrowhead shows periostin-positive PDL tissue. Nuclei were stained with hematoxylin. Bars = 100 μm. All images are shown using horizontal sections, and are representatives of eight independent experiments. D, dentin; PDL, periodontal ligament.

Okada, 2001; Murakami et al., 2003; Murakami, 2011), growth factors or proteins including platelet-derived growth factor (PDGF), BMP2, insulin-like growth factor (IGF), and transforming growth factor-β (TGF-β) also induce osteogenesis and have therapeutic potential in the regeneration of periodontal tissues (Wang, 1993; Graves & Cochran, 1994; McKay, Peckham, & Badura, 2007; Bashutski & Wang, 2009). However, it is known that a large amount of growth factor or protein must be locally administered for bone regeneration in large tissue defects. In fact, clinical results have shown that low concentrations of TGF-β and BMP2 do not produce the expected bone-forming effects (Wu, Bitzer, Ju, Mundel, & Böttinger, 2005; Gautschi, Frey, & Zellweger, 2007; Woo, 2012). Taken together, these reports indicate that regenerative therapies using a large amount of growth factors or recombinant proteins show effective biological activity, but it is difficult to apply such approaches clinically because they are extremely expensive and may be associated with some side effects. Therefore, we have investigated a periodontal tissue regeneration therapy using compounds that can act as alternatives to growth factors, and have focused on the inhibition of JNK phosphorylation.

In the present study, SP600125 promoted the formation of mineralized nodules and the expression of bone-related genes in HPDLSCs, suggesting the involvement of the inhibition of JNK signaling in regulating the osteoblastic differentiation of PDLSCs. Furthermore, SP600125 promoted the BMP2 expression and the phosphorylation of Smad1/5/8, and by inhibiting these promoting effects, SP600125-induced osteoblast differentiation was suppressed. Smad1, Smad5, and Smad8, which are regulated by BMP proteins such as BMP2 and BMP4, are known to play critical roles as transcriptional regulators in osteoblastogenesis and bone metabolism (Nishimura et al., 1998; Fujii et al., 1999; Kawai et al., 2000). In addition, genetic and biochemical studies performed to date indicate that Smad1/5/8 signaling regulates the expression and functions of several transcription factors that are essential for osteoblastic differentiation (Nishimura et al., 2008). Wang et al. reported that Smad1/5/8 signaling participates in enhancing the osteogenic differentiation of PDLSCs (Wang, Li, Ye, He, & Song, 2020). These reports and our findings indicate that SP600125 would promote osteoblastic differentiation of HPDLSCs through BMP2-Smad1/5/8 signaling.

Based on the observations in the present study, the effect of SP600125 on bone regeneration in vivo was examined using a rat periodontal defect model. We demonstrated that SP600125 induced the regeneration of alveolar bone 2 weeks after application into periodontal defects. In addition, the newly formed bone induced by SP600125 strongly expressed osterix, which is an osteoprogenitor marker. In a previous study, osterix knockout mice showed severe impairment of bone formation and osteoblastogenesis (Nakashima et al., 2002), indicating that osterix is an essential transcription factor for bone development. These findings suggest that the alveolar bone regenerated by SP600125 is rich in osteoprogenitors and that SP600125 may have high potential to regenerate such bone. Furthermore, our current study revealed that SP600125 induces the regeneration of PDL tissue that are regularly oriented like "Sharpey's fibers" and express PDL-related markers such as periostin and scleraxis in a rat periodontal defect model. Periostin was reported to regulate collagen fibrillogenesis, thus maintaining correct collagen fibril formation and maturation in heart valves, skin, and tendon; it is also known as a PDL-specific marker (Horiuchi et al., 1999; Romanos, Asnani, Hingorani, & Deshmukh, 2013). Scleraxis is expressed in tendon progenitor populations and mature tendons (Brent, Schweitzer, & Tabin, 2003), and is also commonly used as a marker for periodontal ligament because PDL has tendon-like features (Pöschke, Krähling, Failing, & Staszyk, 2018). Therefore, SP600125 may contribute to the regeneration of the entire periodontal tissue by regenerating not only alveolar bone but also PDL tissue.

In this study, we identified JNK inhibition as a novel method that promotes the regeneration of periodontal tissues. Our findings may lead to the development of a novel periodontal regeneration therapy.

Funding information

JSPS KAKENHI grant numbers JP17H01598, JP17H04385, JP18K19651, and JP19K19002.

CRediT authorship contribution statement

Hiroshi Kaneko: Conceptualization, Methodology, Validation, Formal analysis, Investigation, Data curation, Writing – original draft. **Daigaku Hasegawa:** Conceptualization, Methodology, Formal analysis, Investigation, Writing – review & editing. **Tomohiro Itoyama:** Methodology, Resources, Formal analysis, Investigation, Writing – original draft. **Shinichiro Yoshida:** Resources, Formal analysis, Data curation, Supervision, Writing – original draft. **Atsushi Tomokiyo:** Formal analysis, Data curation, Supervision, Funding acquisition, Writing – original draft. **Sayuri Hamano:** Formal analysis, Data curation, Supervision, Writing – original draft. **Hideki Sugii:** Formal analysis, Data curation, Supervision, Writing – original draft. **Hidefumi Maeda:** Conceptualization, Writing – review & editing, Resources, Supervision, Project administration, Funding acquisition. All authors read and approved the final manuscript.

Declaration of Competing Interest

The authors have no conflicts of interest associated with this manuscript.

Acknowledgments

We thank Drs. Arima, Nozu, Fujino, Ono, Ipposhi, Yamashita, Safwan, Adachi, Kadowaki, Sugiura, Tomita, and Anas for their great support in this work. We also thank Edanz Group (www.edanzediting.com/ac) for editing a draft of this manuscript. This work was supported by JSPS KAKENHI grant numbers JP17H01598, JP17H04385, JP18K19651, and JP19K19002.

Appendix A. Supporting information

Supplementary data associated with this article can be found in the online version at doi:10.1016/j.archoralbio.2021.105323.

References

Bashutski, J. D., & Wang, H. L. (2009). Periodontal and endodontic regeneration. *Journal of Endodontics, 35*(3), 321–328. https://doi.org/10.1016/j.joen.2008.11.023

Beertsen, W., McCulloch, C. A., & Sodek, J. (1997). The periodontal ligament: a unique, multifunctional connective tissue. *Periodontology 2000, 13*, 20–40. https://doi.org/10.1111/j.1600-0757.1997.tb00094.x

Brent, A. E., Schweitzer, R., & Tabin, C. J. (2003). A somitic compartment of tendon progenitors. *Cell, 113*(2), 235–248. https://doi.org/10.1016/s0092-8674(03)00268-x

Chen, Y. R., Meyer, C. F., & Tan, T. H. (1996). Persistent activation of c-Jun N-terminal kinase 1 (JNK1) in gamma radiation-induced apoptosis. *The Journal of Biological Chemistry, 271*(2), 631–634. https://doi.org/10.1074/jbc.271.2.631

Davis, R. J. (2000). Signal transduction by the JNK group of MAP kinases. *Cell, 103*(2), 239–252. https://doi.org/10.1016/s0092-8674(00)00116-1

Freeman, E. (1994). Peridontium. In A. R. Ten Cate (Ed.), *Oral Histology: Development, Structure, and Function* (pp. 276–312). St. Louis: Mosby.

Fujii, M., Takeda, K., Imamura, T., Aoki, H., Sampath, T. K., Enomoto, S., … Miyazono, K. (1999). Roles of bone morphogenetic protein type I receptors and Smad proteins in osteoblast and chondroblast differentiation. *Molecular Biology of the Cell, 10*(11), 3801–3813. https://doi.org/10.1091/mbc.10.11.3801

Fujii, S., Maeda, H., Wada, N., Tomokiyo, A., Saito, M., & Akamine, A. (2008). Investigating a clonal human periodontal ligament progenitor/stem cell line in vitro and in vivo. *Journal of Cellular Physiology, 215*(3), 743–749. https://doi.org/10.1002/jcp.21359

Gautschi, O. P., Frey, S. P., & Zellweger, R. (2007). Bone morphogenetic proteins in clinical applications. *ANZ Journal of Surgery, 77*(8), 626–631. https://doi.org/10.1111/j.1445-2197.2007.04175.x

Ge, C., Xiao, G., Jiang, D., & Franceschi, R. T. (2007). Critical role of the extracellular signal-regulated kinase-MAPK pathway in osteoblast differentiation and skeletal development. *The Journal of Cell Biology, 176*(5), 709–718. https://doi.org/10.1083/jcb.200610046

Graves, D. T., & Cochran, D. L. (1994). Periodontal regeneration with polypeptide growth factors. *Current Opinion in Periodontology*, 178–186.

Guo, C., Wang, S. L., Xu, S. T., Wang, J. G., & Song, G. H. (2015). SP600125 reduces lipopolysaccharide-induced apoptosis and restores the early-stage differentiation of osteoblasts inhibited by LPS through the MAPK pathway in MC3T3-E1 cells. *International Journal of Molecular Medicine, 35*(5), 1427–1434. https://doi.org/10.3892/ijmm.2015.2130

Guo, Y. L., Baysal, K., Kang, B., Yang, L. J., & Williamson, J. R. (1998). Correlation between sustained c-Jun N-terminal protein kinase activation and apoptosis induced by tumor necrosis factor-alpha in rat mesangial cells. *The Journal of Biological Chemistry, 273*(7), 4027–4034. https://doi.org/10.1074/jbc.273.7.4027

Hasegawa, D., Hasegawa, K., Kaneko, H., Yoshida, S., Mitarai, H., Arima, M., … Maeda, H. (2020). MEST regulates the stemness of human periodontal ligament stem cells. *Stem Cells International, 2020*, Article 9672673. https://doi.org/10.1155/2020/9672673

Hasegawa, D., Wada, N., Maeda, H., Yoshida, S., Mitarai, H., Tomokiyo, A., … Akamine, A. (2015). Wnt5a induces collagen production by human periodontal ligament cells through TGFβ1-mediated upregulation of periostin expression. *Journal of Cellular Physiology, 230*(11), 2647–2660. https://doi.org/10.1002/jcp.24950

Hasegawa, D., Wada, N., Yoshida, S., Mitarai, H., Arima, M., Tomokiyo, A., … Maeda, H. (2018). Wnt5a suppresses osteoblastic differentiation of human periodontal ligament stem cell-like cells via Ror2/JNK signaling. *Journal of Cellular Physiology, 233*(2), 1752–1762. https://doi.org/10.1002/jcp.26086

Horiuchi, K., Amizuka, N., Takeshita, S., Takamastu, H., Katsuura, M., Ozawa, H., … Kudo, A. (1999). Identification and characterization of a novel protein, periostin, with restricted expression to periosteum and periodontal ligament and increased expression by transforming growth factor beta. *Journal of Bone and Mineral Research, 14*(7), 1239–1249. https://doi.org/10.1359/jbmr.1999.14.7.1239

Huang, Y. F., Lin, J. J., Lin, C. H., Su, Y., & Hung, S. C. (2012). c-Jun N-terminal kinase 1 negatively regulates osteoblastic differentiation induced by BMP2 via phosphorylation of Runx2 at Ser104. *Journal of Bone and Mineral Research, 27*(5), 1093–1105. https://doi.org/10.1002/jbmr.1548

Ichiyama, K., Sekiya, T., Inoue, N., Tamiya, T., Kashiwagi, I., Kimura, A., … Yoshimura, A. (2011). Transcription factor Smad-independent T helper 17 cell induction by transforming-growth factor-β is mediated by suppression of eomesodermin. *Immunity, 34*(5), 741–754. https://doi.org/10.1016/j.immuni.2011.02.021

Iwasaki, K., Akazawa, K., Nagata, M., Komaki, M., Honda, I., Morioka, C., … Morita, I. (2019). The fate of transplanted periodontal ligament stem cells in surgically created periodontal defects in rats. *International Journal of Molecular Sciences, 20*(1), 192. https://doi.org/10.3390/ijms20010192

Kawai, S., Faucheu, C., Gallea, S., Spinella-Jaegle, S., Atfi, A., Baron, R., & Roman, S. R. (2000). Mouse smad8 phosphorylation downstream of BMP receptors ALK-2, ALK-3, and ALK-6 induces its association with Smad4 and transcriptional activity. *Biochemical and Biophysical Research Communications, 271*(3), 682–687. https://doi.org/10.1006/bbrc.2000.2704

King, G. N., King, N., Cruchley, A. T., Wozney, J. M., & Hughes, F. J. (1997). Recombinant human bone morphogenetic protein-2 promotes wound healing in rat periodontal fenestration defects. *Journal of Dental Research, 76*(8), 1460–1470. https://doi.org/10.1177/00220345970760080801

Kyriakis, J. M., & Avruch, J. (2001). Mammalian mitogen-activated protein kinase signal transduction pathways activated by stress and inflammation. *Physiological Reviews, 81*(2), 807–869. https://doi.org/10.1152/physrev.2001.81.2.807

Maeda, H., Wada, N., Nakamuta, H., & Akamine, A. (2004). Human periapical granulation tissue contains osteogenic cells. *Cell and Tissue Research, 315*(2), 203–208. https://doi.org/10.1007/s00441-003-0832-z

McKay, W. F., Peckham, S. M., & Badura, J. M. (2007). A comprehensive clinical review of recombinant human bone morphogenetic protein-2 (INFUSE Bone Graft). *International Orthopaedics, 31*(6), 729–734. https://doi.org/10.1007/s00264-007-0418-6

Miyazono, K., Maeda, S., & Imamura, T. (2005). BMP receptor signaling: transcriptional targets, regulation of signals, and signaling cross-talk. *Cytokine & Growth Factor Reviews, 16*(3), 251–263. https://doi.org/10.1016/j.cytogfr.2005.01.009

Murakami, S. (2011). Periodontal tissue regeneration by signaling molecule(s): what role does basic fibroblast growth factor (FGF-2) have in periodontal therapy? *Periodontology 2000, 56*(1), 188–208. https://doi.org/10.1111/j.1600-0757.2010.00365.x

Murakami, S., Takayama, S., Kitamura, M., Shimabukuro, Y., Yanagi, K., & Ikezawa, K. (2003). Recombinant human basic fibroblast growth factor (bFGF) stimulates periodontal regeneration in class II furcation defects created in beagle dogs. *Journal of Periodontal Research, 38*(1), 97–103. https://doi.org/10.1034/j.1600-0765.2003.00640.x

Nagata, M., Iwasaki, K., Akazawa, K., Komaki, M., Yokoyama, N., Izumi, Y., & Morita, I. (2017). Conditioned medium from periodontal ligament stem cells enhances periodontal regeneration. *Tissue Engineering Part A, 23*(9–10), 367–377. https://doi.org/10.1089/ten.TEA.2016.0274

Nakashima, K., Zhou, X., Kunkel, G., Zhang, Z., Deng, J. M., Behringer, R. R., & de Crombrugghe, B. (2002). The novel zinc finger-containing transcription factor osterix is required for osteoblast differentiation and bone formation. *Cell, 108*(1), 17–29. https://doi.org/10.1016/s0092-8674(01)00622-5

Nishimura, R., Hata, K., Ikeda, F., Ichida, F., Shimoyama, A., Matsubara, T., … Yoneda, T. (2008). Signal transduction and transcriptional regulation during mesenchymal cell differentiation. *Journal of Bone and Mineral Metabolism, 26*(3), 203–212. https://doi.org/10.1007/s00774-007-0824-2

Nishimura, R., Kato, Y., Chen, D., Harris, S. E., Mundy, G. R., & Yoneda, T. (1998). Smad5 and DPC4 are key molecules in mediating BMP-2-induced osteoblastic differentiation of the pluripotent mesenchymal precursor cell line C2C12. *The Journal of Biological Chemistry, 273*(4), 1872–1879. https://doi.org/10.1074/jbc.273.4.1872

Papadopoulou, A., Iliadi, A., Eliades, T., & Kletsas, D. (2017). Early responses of human periodontal ligament fibroblasts to cyclic and static mechanical stretching. *European Journal of Orthodontics, 39*(3), 258–263.

Pöschke, A., Krähling, B., Failing, K., & Staszyk, C. (2018). Molecular characteristics of the equine periodontal ligament. *Frontiers in Veterinary Science, 11*(4), 235. https://doi.org/10.3389/fvets.2017.00235

Rath, B., Nam, J., Deschner, J., Schaumburger, J., Tingart, M., Grässel, S., … Agarwal, S. (2011). Biomechanical forces exert anabolic effects on osteoblasts by activation of SMAD 1/5/8 through type 1 BMP receptor. *Biorheology, 48*(1), 37–48. https://doi.org/10.3233/BIR-2011-0580

Romanos, G. E., Asnani, K. P., Hingorani, D., & Deshmukh, V. L. (2013). PERIOSTIN: role in formation and maintenance of dental tissues. *Journal of Cellular Physiology, 229*(5), 1–5. https://doi.org/10.1002/jcp.24491

Seino, M., Okada, M., Sakaki, H., Takeda, H., Watarai, H., Suzuki, S., … Kitanaka, C. (2016). Time-staggered inhibition of JNK effectively sensitizes chemoresistant ovarian cancer cells to cisplatin and paclitaxel. *Oncology Reports, 35*(1), 593–601. https://doi.org/10.3892/or.2015.4377

Seo, B. M., Miura, M., Gronthos, S., Bartold, P. M., Batouli, S., Brahim, J., … Shi, S. (2004). Investigation of multipotent postnatal stem cells from human periodontal ligament. *Lancet, 364*(9429), 149–155. https://doi.org/10.1016/S0140-6736(04)16627-0

Takayama, S., Murakami, S., Shimabukuro, Y., Kitamura, M., & Okada, H. (2001). Periodontal regeneration by FGF-2 (bFGF) in primate models. *Journal of Dental Research, 80*(12), 2075–2079. https://doi.org/10.1177/00220345010800121001

Wang, E. A. (1993). Bone morphogenetic proteins (BMPs): therapeutic potential in healing bony defects. *Trends in Biotechnology, 11*(9), 379–383. https://doi.org/10.1016/0167-7799(93)90096-R

Wang, M., Li, J., Ye, Y., He, S., & Song, J. (2020). SHED-derived conditioned exosomes enhance the osteogenic differentiation of PDLSCs via Wnt and BMP signaling in vitro. *Differentiation, 111*, 1–11. https://doi.org/10.1016/j.diff.2019.10.003

Weston, C. R., & Davis, R. J. (2002). The JNK signal transduction pathway. *Current Opinion in Genetics & Development, 12*(1), 14–21. https://doi.org/10.1016/s0959-437x(01)00258-1

Woo, E. J. (2012). Adverse events reported after the use of recombinant human bone morphogenetic protein 2. *Journal of Oral and Maxillofacial Surgery, 70*(4), 765–767. https://doi.org/10.1016/j.joms.2011.09.008

Wu, D. T., Bitzer, M., Ju, W., Mundel, P., & Böttinger, E. P. (2005). TGF-beta concentration specifies differential signaling profiles of growth arrest/differentiation and apoptosis in podocytes. *Journal of the American Society of Nephrology, 16*(11), 3211–3221. https://doi.org/10.1681/ASN.2004121055